Journal of the Nigerian Association of Mathematical Physics
***Volume 30, (May, 2015*), pp169 – 180**
© J. of NAMP

Separation of Regional-Residual Anomaly Using Least Square Polynomial Fitting Method

[1]Layade G.O., [2]Adebo B.A., [3]Olurin O.T. and [4]Ganiyu O.M.

[1,3,4]Department of Physics, Federal University of Agriculture, Abeokuta Nigeria
[2]Department of Physics, Lead City University, Ibadan.

Abstract

This paper presents quantitative application of Least-Square Polynomial fitting method in regional-residual separation. The study area covered geographical coordinate between latitude 8˚06΄70˝N and 8˚06΄98.7''north and longitude 4˚14΄28.2˝E and 4˚14΄56.9˝ east of the Aeromagnetic maps of the region. The data were obtained by digitizing the maps of the above areas, picking the Total magnetic values along the profile line, processed and analyzed. The result of the residual separation revealed that the area is underlain by a NE-SW regional trend, characterized by basement complex with a weak amplitude of approximately – 85.73l nT. The regional magnetic anomaly map shows that the southern part of the map is suspected to be sedimentary basin, which is W-E trending, an indication of smoother magnetic field and it masked off the effects of the stronger magnetic basement. The basement complex underlies between the north and south of the study area comprises of broader area of outcrops.

Keywords: Aeromagnetic map, Regional and Residual fields, basement complex, Polynomial fitting

1.0 Introduction

Aeromagnetic is the collection of magnetic data by small aircraft over a large area expanse of area (which may or not accessible) and interpreting the data using several techniques. It is a method of arriving at ore deposited within geographic area [1]. Aeromagnetic data records variation in the magnitude of the earth's magnetic field in order to detect local changes in the properties of the underlying geology. The magnetic method of exploring the surface is used to either map or locate rock type that contain varying amount of magnetic susceptible material [2]. Magnetic data are commonly used to map thin magnetic sheets and /or contact such as faults in the basement that may control the depositional history of sedimentary basin. The existence of various minerals beneath the earth crust has over the years led to the invention of various ways of determining these minerals and their position within the earth crust [3, 4]. A general approach that has over the years been used to study the existence of minerals in an area is known as the geophysical survey.

2.0 Method and Theoretical Analysis

2.1 Location and Geology of the Study Area

The study area covered geographical coordinate between latitude 8˚06΄70˝N and 8˚06΄98.7''north and longitude 4˚14΄28.2˝E and 4˚14΄56.9˝ east of Ogbomoso-regionaeromagnetic map in Oyo state, south-western part of Nigeria. The geology of the study area consists of Precambrian rocks that are typical for the basement complex of Nigeria [5]. The major rock associated with Ogbomoso area form part of the Proterozoic schist belts of Nigeria, which are predominantly, developed in the western half of the country.

In terms of structural features, lithology and mineralization, the schist belts show considerable similarities to the Achaean Green Stone belts. However, the latter usually contain much larger proportions of mafic and ultra-mafic bodies and assemblages of lower metamorphic grade [5,6]. The gneiss complex which underlies the northern and southern part of the Ogbomoso district comprises a considerable broader area of outcrops. Locally, the rock sequence composes of basically weathered quartzite and older granites. The minerals found in this area constitute mostly amphibolites, amphibole schist, meta ultra mafites and meta pelites. Extensive psammitic units and minor meta pelite can also be found which consist of quartzites and quartz schist.

Corresponding author: Layade, G.O., E-mail: layadeoluyinka018@gmail.com, Tel.: +2348139437356

The rocks of the district may be broadly grouped into gneiss-migmatite complex or amphibolite complex, Meta sedimentary assemblages and intrusive suite of granitic rocks.
A variety of minor rock types are also related to these units. The minor rocks includeGarnet-quartz-chlorite bodies, biotites-garnet rock, syenitic bodies, and dolerites [5,7]. It overlies the western upland region of the Nigeria highland plateaux with average altitude between 1000m and 1500m above mean sea level [8]. The drainage type is intrinsically dendrites.

2.2 Map Digitization and Data Enhancement

The aeromagnetic map of the study area was manually digitized with 55*x*55 grids along longitude(x) and latitude(y) coordinates. Magnetic intensity values (z values) were obtained for every *x-axis* corresponding to*y-axis*. The *xyz* values are tabulated and then enhanced through the process of regional anomaly removal and reduction to pole. The residual magnetic anomaly was processed through the Geosoft Oasis Montaj^{TM} 7.0, a menu-driven interactive computer programme, which places each magnetic data point according to their longitude and latitude bearing and thereafter produces contour and intensity maps that represent the data.

2.3 The Least-Square Polynomial Fitting Theory

The least square method was applied because the study area seemed adequate and reasonable to assume that the regional field is a first polynomial surface [9]. All the regional were therefore calculated as a two dimensional first – degree polynomial surface. To eliminate the regional field, a plane surface was fitted to the data by multiple regression least-squares criteria established by the mathematical concept[9-11]. The polynomial coefficients were used to compute the regional map of the study area. The resultant map is shown Figure2. The data were processed with an automated contouring software programme which generated the residual field intensity map of the study area shown in Figure.3, while graphical result of the separated values are contained in Figures 4-11.

Generalizing from a straight line (i.e., first degree polynomial) to a kth degree polynomial

$$y = a_0 + a_1 x + \ldots + a_k x^k, \tag{1}$$

the residual is given by

$$R^2 \equiv \sum_{i=1}^{n} \left[y_i - \left(a_0 + a_1 x_i + \ldots + a_k x_i^k \right) \right]^2. \tag{2}$$

The partial derivatives (again dropping superscripts) are

$$\frac{\partial (R^2)}{\partial a_0} = -2 \sum_{i=1}^{n} \left[y - \left(a_0 + a_1 x + \ldots + a_k x^k \right) \right] = 0 \tag{3}$$

$$\frac{\partial (R^2)}{\partial a_1} = -2 \sum_{i=1}^{n} \left[y - \left(a_0 + a_1 x + \ldots + a_k x^k \right) \right] x = 0 \tag{4}$$

$$\frac{\partial (R^2)}{\partial a_k} = -2 \sum_{i=1}^{n} \left[y - \left(a_0 + a_1 x + \ldots + a_k x^k \right) \right] x^k = 0. \tag{5}$$

These lead to the equations

$$a_0 n + a_1 \sum_{i=1}^{n} x_i + \ldots + a_k \sum_{i=1}^{n} x_i^k = \sum_{i=1}^{n} y_i \tag{6}$$

$$a_0 \sum_{i=1}^{n} x_i + a_1 \sum_{i=1}^{n} x_i^2 + \ldots + a_k \sum_{i=1}^{n} x_i^{k+1} = \sum_{i=1}^{n} x_i y_i \tag{7}$$

$$a_0 \sum_{i=1}^{n} x_i^k + a_1 \sum_{i=1}^{n} x_i^{k+1} + \ldots + a_k \sum_{i=1}^{n} x_i^{2k} = \sum_{i=1}^{n} x_i^k y_i \tag{8}$$

or, in matrix form

$$\begin{bmatrix} n & \sum_{i=1}^{n} x_i & \cdots & \sum_{i=1}^{n} x_i^k \\ \sum_{i=1}^{n} x_i & \sum_{i=1}^{n} x_i^2 & \cdots & \sum_{i=1}^{n} x_i^{k+1} \\ \vdots & \vdots & \ddots & \vdots \\ \sum_{i=1}^{n} x_i^k & \sum_{i=1}^{n} x_i^{k+1} & \cdots & \sum_{i=1}^{n} x_i^{2k} \end{bmatrix} \begin{bmatrix} a_0 \\ a_1 \\ \vdots \\ a_k \end{bmatrix} = \begin{bmatrix} \sum_{i=1}^{n} y_i \\ \sum_{i=1}^{n} x_i y_i \\ \vdots \\ \sum_{i=1}^{n} x_i^k y_i \end{bmatrix}. \tag{9}$$

This is a Vandermonde matrix [12]. We can also obtain the matrix for a least squares fit by writing

$$\begin{bmatrix} 1 & x_1 & \cdots & x_1^k \\ 1 & x_2 & \cdots & x_2^k \\ \vdots & \vdots & \ddots & \vdots \\ 1 & x_n & \cdots & x_n^k \end{bmatrix} \begin{bmatrix} a_0 \\ a_1 \\ \vdots \\ a_k \end{bmatrix} = \begin{bmatrix} y_1 \\ y_2 \\ \vdots \\ y_n \end{bmatrix}. \tag{10}$$

Pre-multiplying both sides by the transpose of the first matrix then gives

$$\begin{bmatrix} 1 & 1 & \cdots & 1 \\ x_1 & x_2 & \cdots & x_n \\ \vdots & \vdots & \ddots & \vdots \\ x_1^k & x_2^k & \cdots & x_n^k \end{bmatrix} \begin{bmatrix} 1 & x_1 & \cdots & x_1^k \\ 1 & x_2 & \cdots & x_2^k \\ \vdots & \vdots & \ddots & \vdots \\ 1 & x_n & \cdots & x_n^k \end{bmatrix} \begin{bmatrix} a_0 \\ a_1 \\ \vdots \\ a_k \end{bmatrix}$$

$$= \begin{bmatrix} 1 & 1 & \cdots & 1 \\ x_1 & x_2 & \cdots & x_n \\ \vdots & \vdots & \ddots & \vdots \\ x_1^k & x_2^k & \cdots & x_n^k \end{bmatrix} \begin{bmatrix} y_1 \\ y_2 \\ \vdots \\ y_n \end{bmatrix}, \tag{11}$$

so

$$\begin{bmatrix} n & \sum_{i=1}^n x_i & \cdots & \sum_{i=1}^n x_i^k \\ \sum_{i=1}^n x_i & \sum_{i=1}^n x_i^2 & \cdots & \sum_{i=1}^n x_i^{k+1} \\ \vdots & \vdots & \ddots & \vdots \\ \sum_{i=1}^n x_i^k & \sum_{i=1}^n x_i^{k+1} & \cdots & \sum_{i=1}^n x_i^{2k} \end{bmatrix} \begin{bmatrix} a_0 \\ a_1 \\ \vdots \\ a_k \end{bmatrix} = \begin{bmatrix} \sum_{i=1}^n y_i \\ \sum_{i=1}^n x_i y_i \\ \vdots \\ \sum_{i=1}^n x_i^k y_i \end{bmatrix}. \tag{12}$$

As before, given n points (x_i, y_i) and fitting with polynomial coefficients a_0, ..., a_k gives

$$\begin{bmatrix} y_1 \\ y_2 \\ \vdots \\ y_n \end{bmatrix} = \begin{bmatrix} 1 & x_1 & x_1^2 & \cdots & x_1^k \\ 1 & x_2 & x_2^2 & \cdots & x_2^k \\ \vdots & \vdots & \vdots & \ddots & \vdots \\ 1 & x_n & x_n^2 & \cdots & x_n^k \end{bmatrix} \begin{bmatrix} a_0 \\ a_1 \\ \vdots \\ a_k \end{bmatrix}, \tag{13}$$

In matrix notation, the equation for a polynomial fit is given by

$$\mathbf{y} = \mathsf{X}\,\mathbf{a}. \tag{14}$$

This can be solved by pre-multiplying by the transpose X^T,

$$\mathsf{X}^T\,\mathbf{y} = \mathsf{X}^T\,\mathsf{X}\,\mathbf{a}. \tag{15}$$

This matrix equation can be solved numerically, or can be inverted directly if it is well formed, to yield the solution vector

$$\mathbf{a} = (\mathsf{X}^T\,\mathsf{X})^{-1}\,\mathsf{X}^T\,\mathbf{y}. \tag{16}$$

Setting $k = 1$ in the above equations reproduces the linear solution.

3.0 Result and Discussion

The main use of any aeromagnetic and their derivative maps in mineral prospecting is to make geological deduction from them, thus from the range of magnetic intensity values of these data, information on subsurface lithology, trend and geological structures can be obtained [10].

3.1 Geological Mapping From Total Magnetic Intensity

The map in Figure1 covers an area of approximately 27.799km by 27.518km and is bounded by 8.15^0Nto 8.40^0 N in latitudes and 4.00^0Nto 4.25^0 E in longitudes. The shaded colour aeromagnetic map of the study area have intensity within the range of 32849.4 nT - 32986.6 nT suggesting contrasting rock types in the basement. The northern region of this map has a basement complex with an intrusion of high magnetic intensity that ranges from 32978.7 nT to 33003.0 nT. There is a demarcation along the latitude 8.25^0 and 8.30^0 between the northern and the southern part of the map that consist of little intrusion with minimum intensity value that ranges from 32892.4 nT to 32917.5 nT characterized by a moderate magnetic intensity that range from 32932.0 nT to 32940.2 nT while the southern zone is characterized by sedimentary basement with a prominent intrusive bodies of low magnetic intensity between 32849.4 nT and 32908.4 nT. Also present is the little intrusion of high magnetic intensity which ranges from 32971.7 nT to 32986.6 nT which may be due to noise, outcrops or cultural source. The Figure 3is the derived residual magnetic intensity map with its contour, which represents the qualitative representation of spatial variation in the magnetic properties of deep basement rocks and structures in the area.

3.2 Geological Mapping from Residual Anomaly

The map in Figure 2 covers an area of approximately 27.799km by 27.518km bounded by 8.15^0Nto 8.40^0 N in latitudes and 4.00^0 to 4.25^0 E in longitudes, The shaded colour map of the residual ranges from -122.6nT to +51.1nT. The residual map reveals that the study area is characterized majorly by sedimentary basement. However, by dividing the map into four quadrants vis-à-vis northwest, northeast, southwest and southeast respectively; The northwest of the map is characterized by weak to moderate amplitude magnetic anomalies that ranges from -13.6nT to 19.8nT with an isolated negative magnetic intensity that ranges from -28.6nT to -13.6nT.In the northeast part of the map an intrusion was observed ranging from -46.4 to -28.6nT and is characterized by a slightly weak to moderate anomaly between -2.3nT and 25.0nTwith little positive intrusive bodies. Southeast part consist of thick sedimentary basement of the map within the range of +2.6nTto+51.1nT of the residual magnetic intensity value, however with some isolated negative anomalies that ranges from -122.6nT to-28.6nT. In the southwest part of the magnetic anomaly map high magnetic anomaly ranges from 4.7nT to 51.1nT with an intrusion of magnetic intensity value between -122.6nT to and 46.4nT may be due to noise or cultural source.

3.3 Geological Mapping from Regional Anomaly

The map of the Regional magnetic intensity in Figure 3 with an amplitude ranging from 32858.7 nT to 32988.9 nT over an area of 27.799 km by27.518 km, bounded by 8.15^0N to 8.40^0N in latitudes and 4.00^0E to 4.25^0 E in longitude. Dividing the map into northwest, northeast, southwest and southeast. The northwest of the map is characterized by moderate intensity that ranges from 32933.8 nT to 32967.3 nT with an isolated intensity that ranges from 32980.2 nT to 32988.9 nT. The northeast zone is sparsely distributed by high magnetic intensity value ranging from 32953.1nT to32980.2nT with intrusive bodies of moderate intensity value between 32911.2nT and 32933.8nT.

The southwest zone of this map is characterized by moderate intensity ranging from 32925.3nT to32941.5nT with an isolated body of high intensity that reflects around the zone, this body has an intensity that ranges from 32980.2nT to 32985 3nT with an intrusion of weak intensity that ranges from 32858.7nT to 32919.7nT.The southeast zone has a moderate intensity that ranges from 32925.3nT to 32937.8nT with intrusion that ranges from 32858.7nT to 32919.7nT and a reflection of high amplitude is clearly seen within this region of the map, this reflections ranges from 32956.6nT to 32988.9nT.

3.4 Discussion

3.4.1 Inferences from Contour Maps

On the residual map in Figure 2, the residual magnetic field are concentrated more in the Northern and Southern portion of the study area. This may be explained that the basement complex outcropping here is not homogeneous mineral-wise in addition to the presence of intrusive bodies in the area with weathered quartzite, while others are grannitic and pegmatitic dyke. This inferred zone may be interpreted as major fracture zones of the weak intensity within thestudy area. The NE-SW lineaments are found more towards the northeast and southwestern part of the study area with some extension in the southwestern part. The high amplitude of the anomalies which out crop across north area is likely to be lunguda basalt. Area showing negative residual anomalies in the study area could be due to the presence of granite-gneiss in the area. They may also be due to the susceptibility variations in the lithology or a combination of both.

In this study, it is assumed that the anomalous magnetic field of the crustal rocks is due to induced magnetization in the area as revealed in Figures 3-4 showing both the residual anomaly map and the regional map of the surveyed area respectively. The residual anomaly in Figure 2 ranging from -122.6 nT to +51.1 nT depicts the anomaly of the earth magnetic field due to sources below the subsurface in N-S trend characterized by sedimentary basin westward with sprockets of igneous intrusion. On the other hand, the regional anomaly map in Figure 3 with intensities ranging from 32858.7 nT to 32988 nT presents the magnetic intrusive materials at the northern part of the area migrating towards the south.

3.4.2 Inferences from Least Square Trend-Line Analysis

The Least-Square polynomial trend analysis was used to fit the magnetic data through which the regional and the residual were separated. Figures 4-11 represent profiles 1-8 of the entire region in both regional and residual anomaly respectively. The graph as plotted using the Microsoft Excel package shows the resulting trend-line equation for each profile. It was observed that profiles 1, 6-8 in Figures 4, 9-11 have their residual after separation largely below the trend line which is an indication of the fact that the anomaly was as a result of the fairly thick sedimentary basin with low magnetization within the range of -1000 nT to -100 nT of the basement complex. On the other hand, the traverses as represented by Figures 5-8 referred to as profiles 2-6 have relatively high residual magnetic anomaly ranging between +40 nT and +100 nT after separation. This suggests that the area within the location must have possessed sprockets of igneous intrusion and weathered metamorphic grains with a good prospect magnetic mineral prospect.

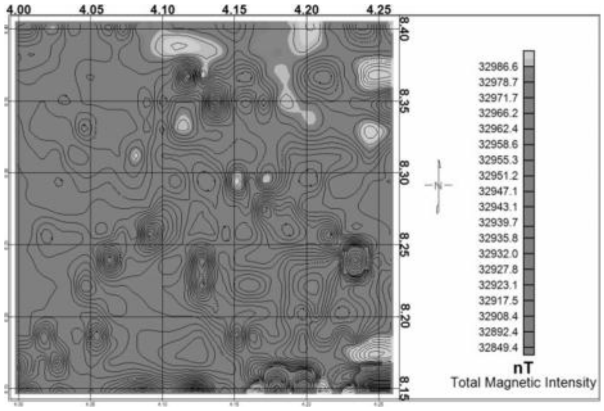

Figure 1: Map for the observed Total Magnetic intensity for the study area.

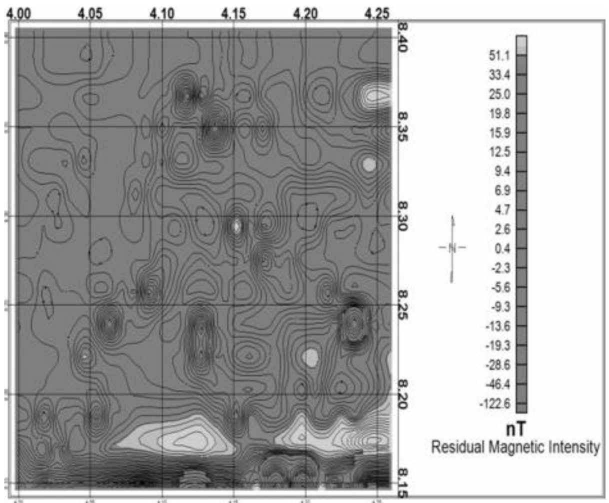

Figure 2: Residual magnetic field intensity with its contour.

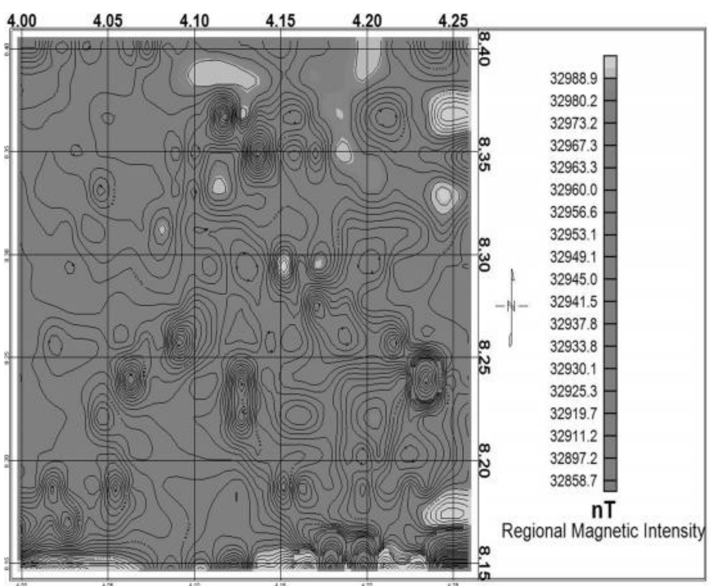

Figure 3: Regional magnetic field intensity with its contour and the Imaging of anomaly due to earth magnetic field.

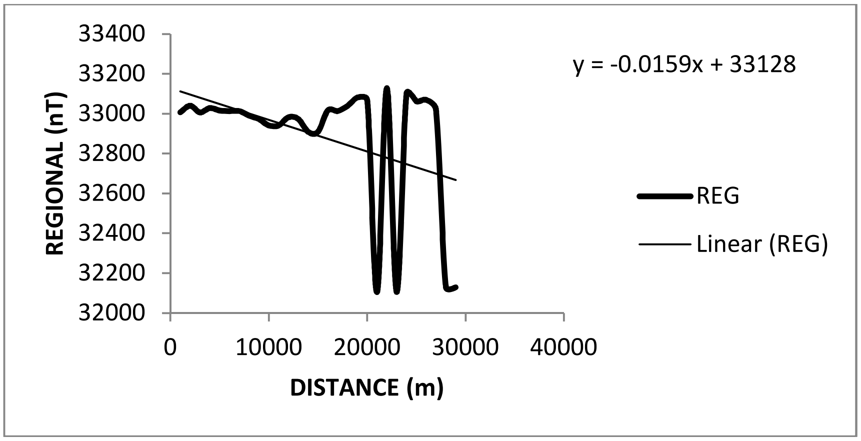

Figure 4a: Graph of Regional field against Distance for profile 1

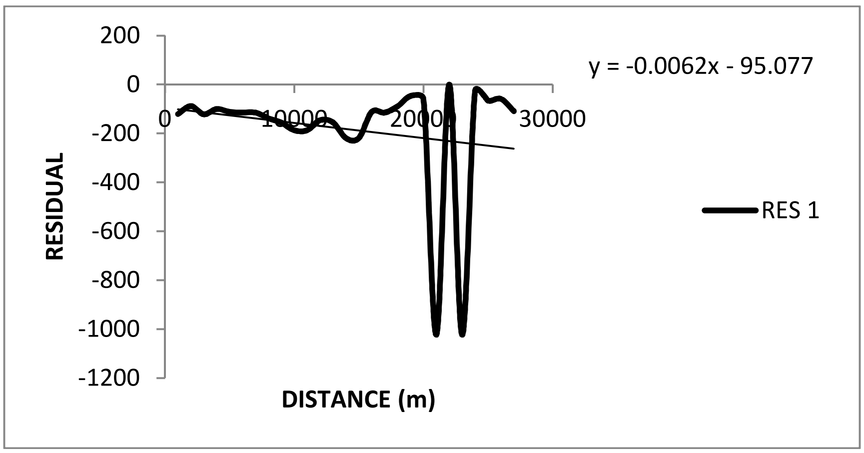

Figure 4b: Graph of Residual field against Distance for profile 1

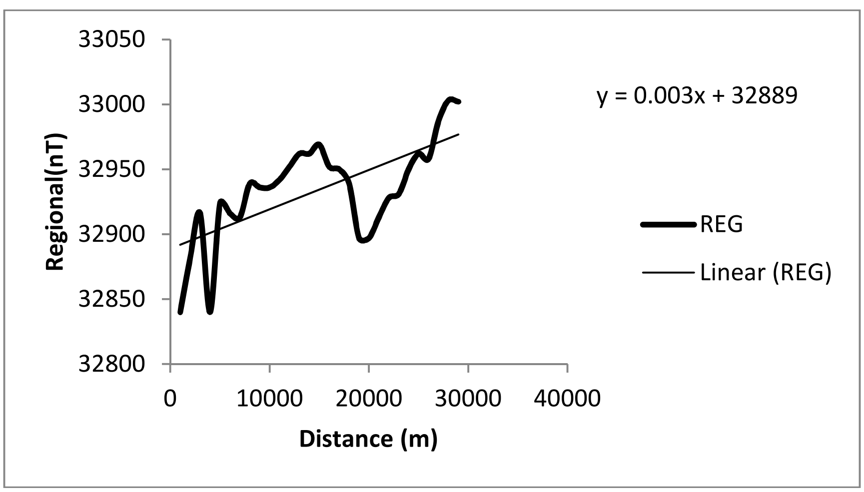

Figure 5a: Graph of Regional field against Distance for profile 2

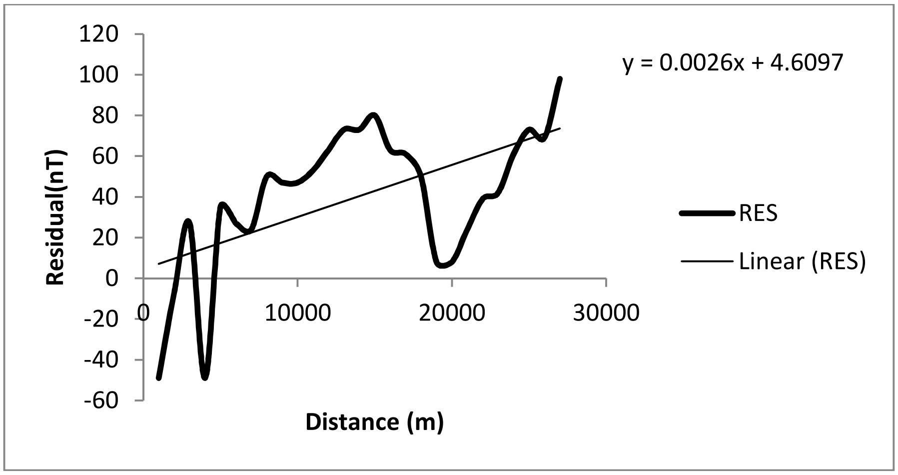

Figure 5b: Graph of Residual field against Distance for profile 2

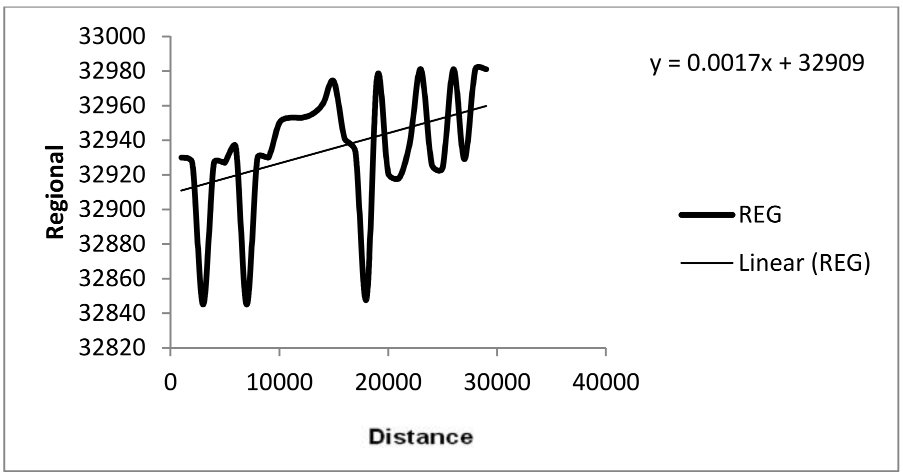

Figure 6a: Graph of Regional field against Distance for profile 3

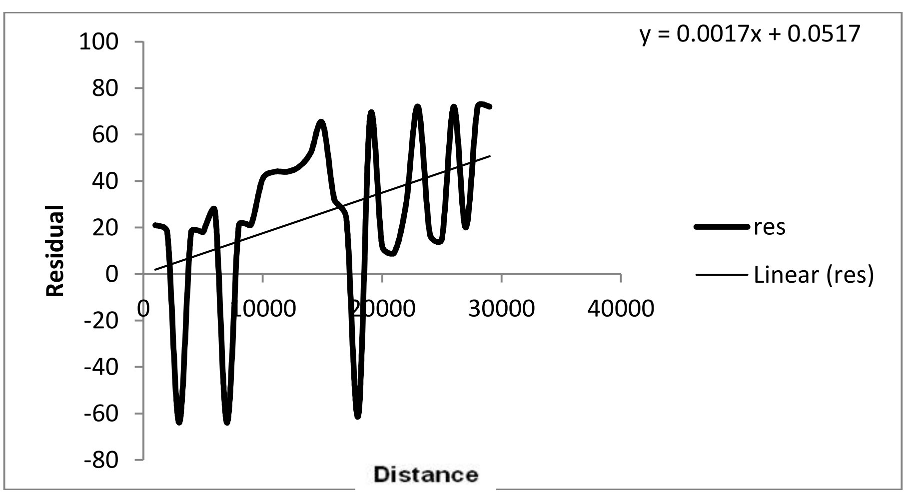

Figure 6b: Graph of Residual field against distance for profile 3

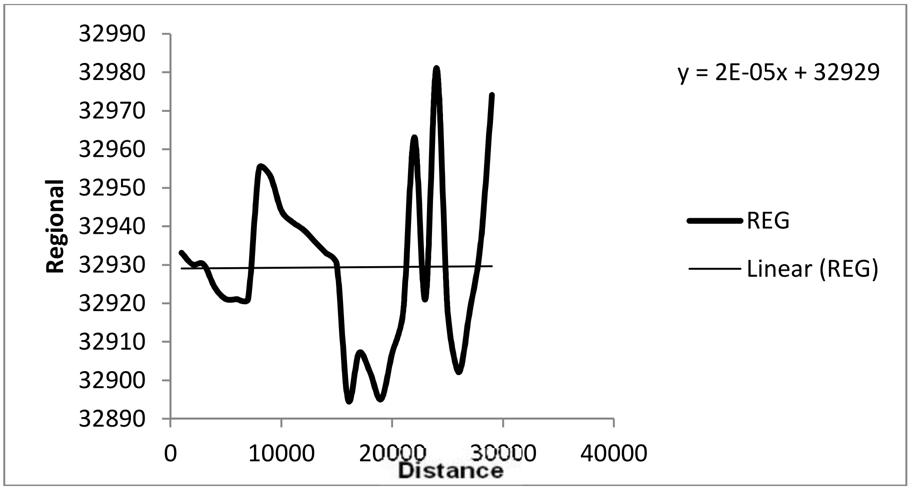

Figure 7a: Graph of regional field against Distance for profile 4

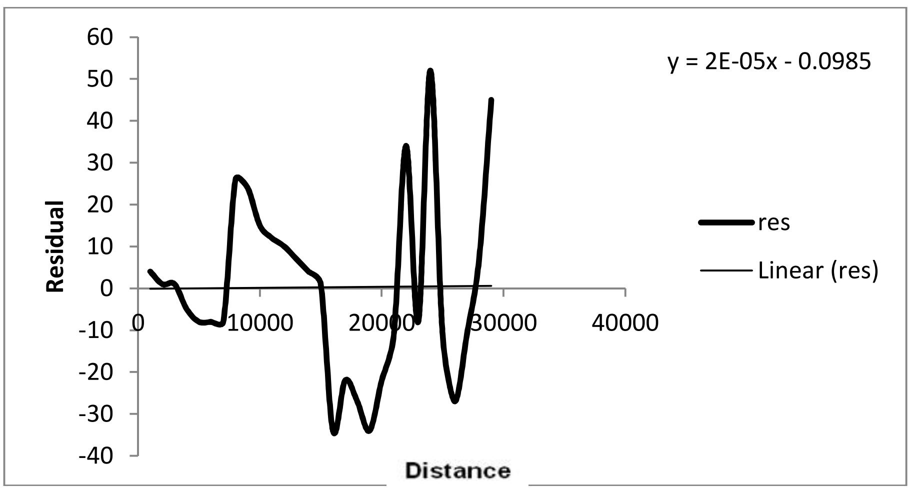

Figure 7b: Graph of residual against distance for profile 4

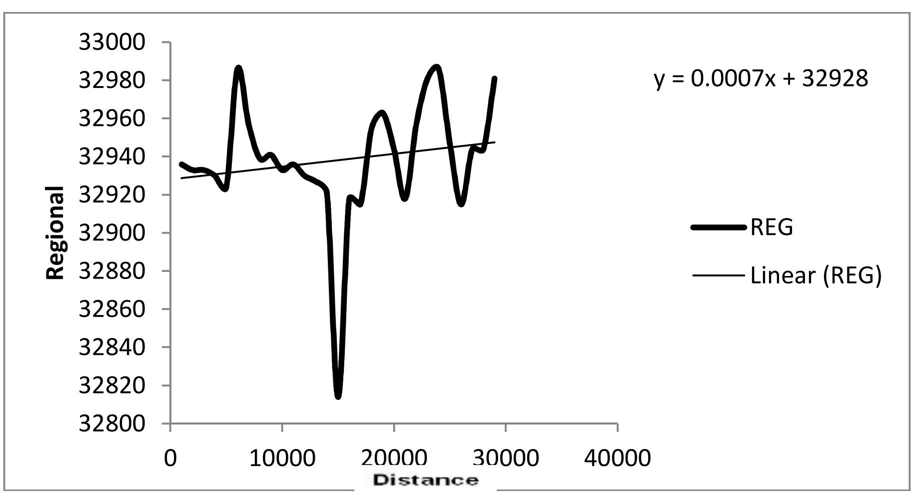

Figure 8a: Graph of regional field against Distance for profile 5

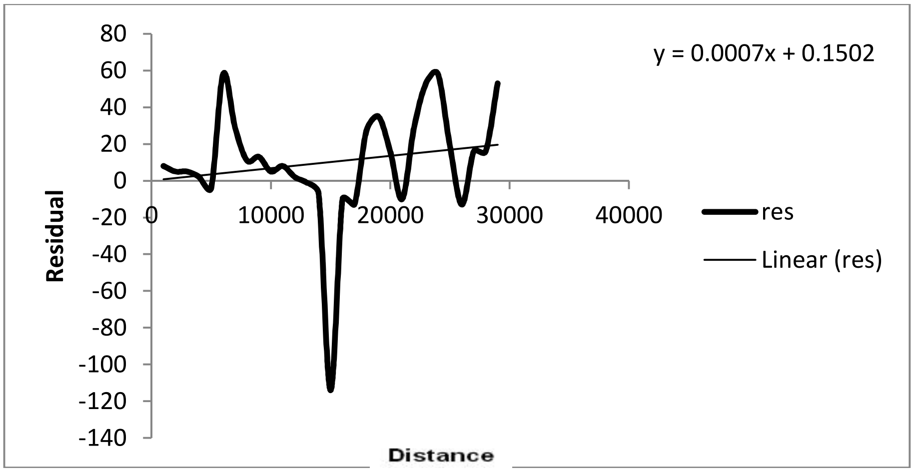

Figure 8b: Graph of residual field against distance for profile 5

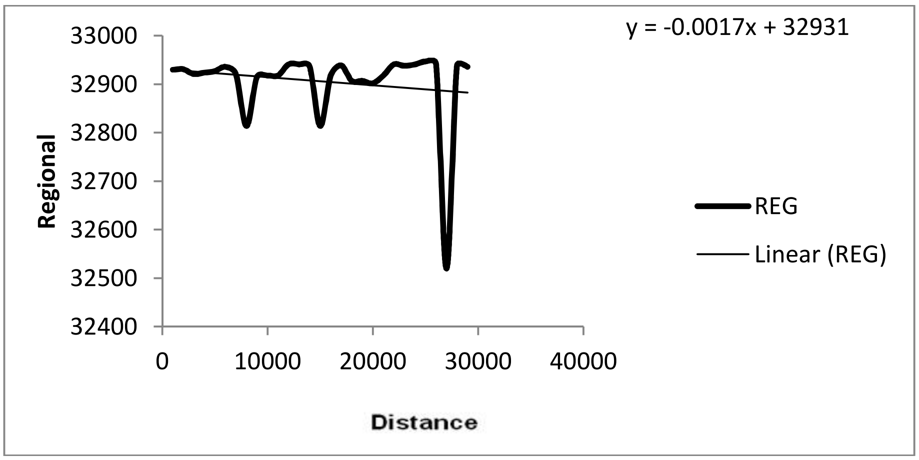

Figure 9a: Graph of regional against Distance for profile 6

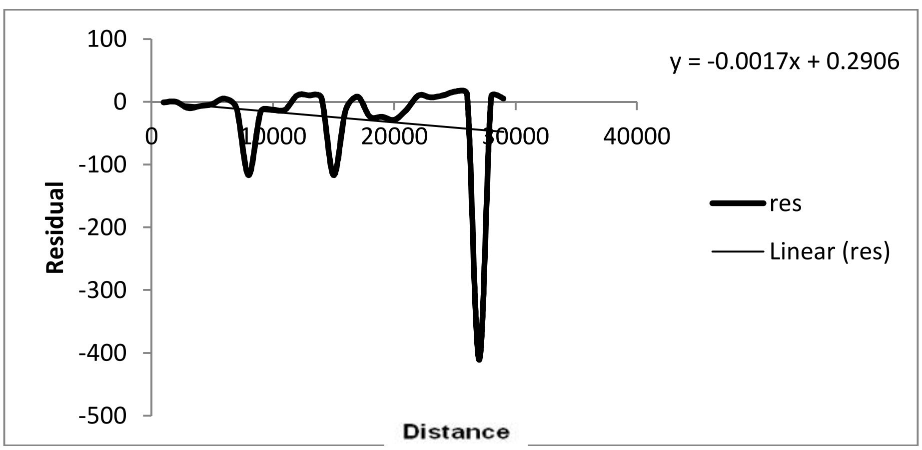

Figure 9b: Graph of residual against distance for profile 6

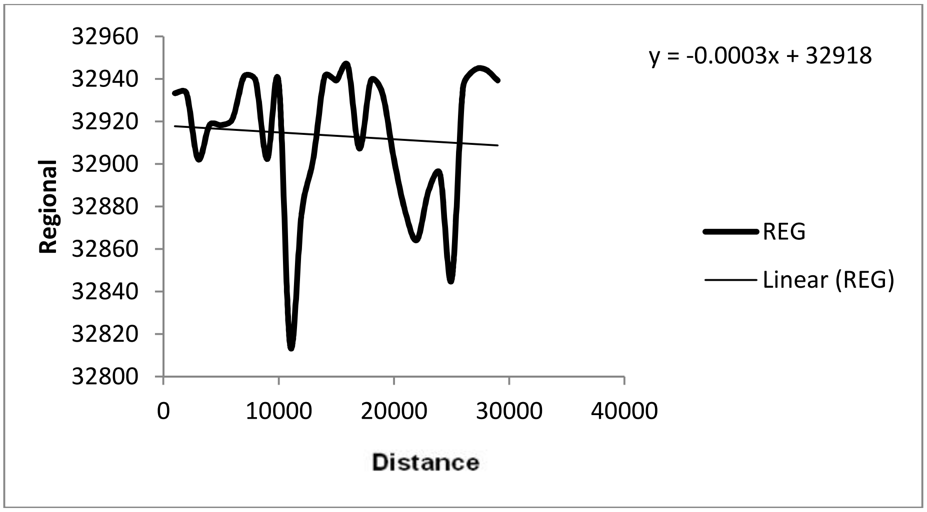

Figure 10a: Graph of Regional against Distance for profile 7

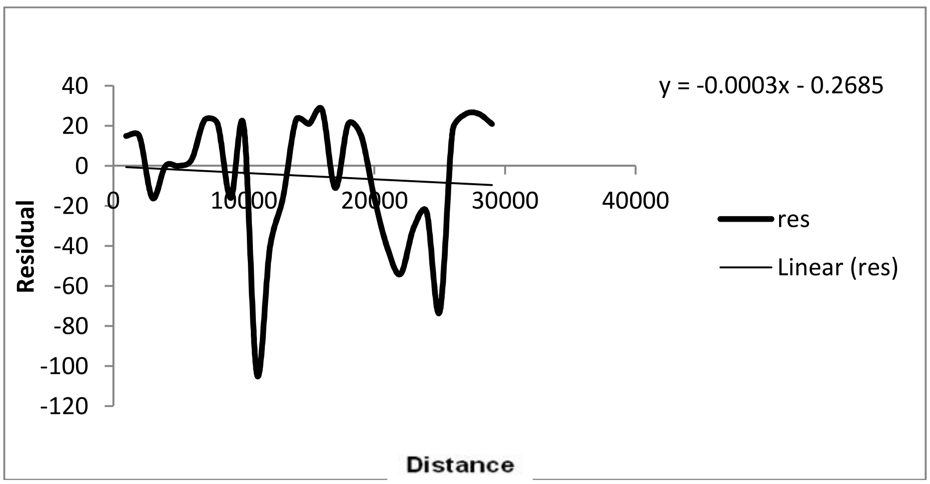

Figure 10b: Graph of residual against distance for profile 7

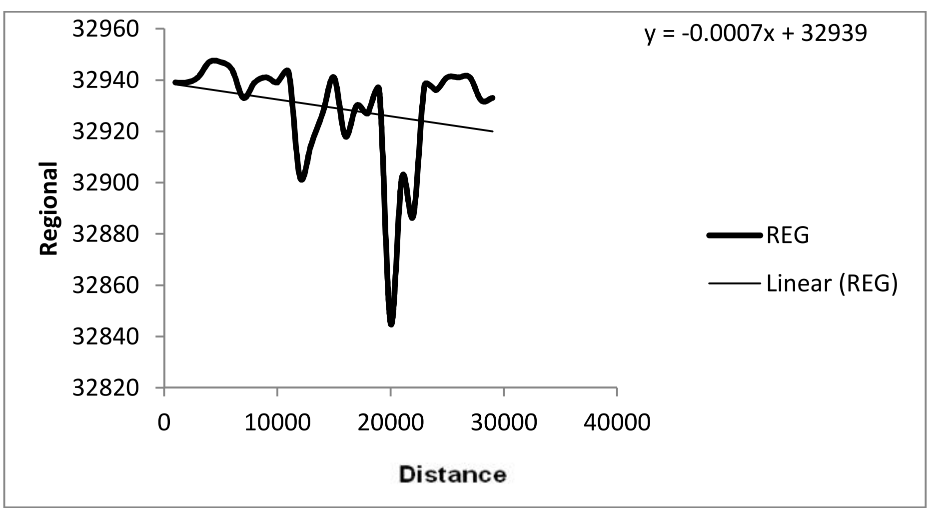

Figure 11a: Graph of Regional against Distance for profile 8

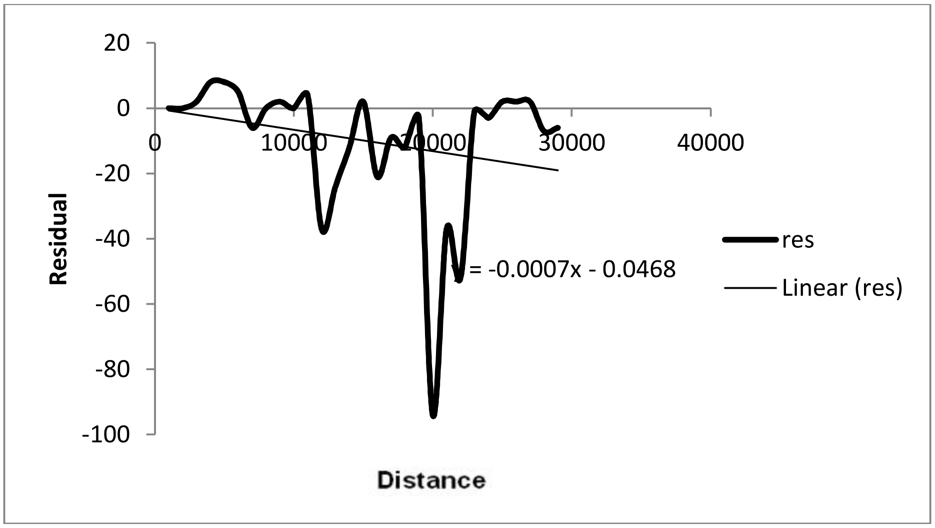

Figure 11b: Graph of residual against distance for profile 8

4.0 Conclusion

The analysis of the digitized aeromagnetic map of the study area using Polynomial fitting method in regional-residual separation produced the residual magnetic anomaly map. The result of the trend analysis by using the derived residual data showed that the area is characterized by basement complex. By magnetic zoning based on anomaly pattern and their distribution, the northern path of the regional map derived from the study area is characterized by basement complex with a broad area of outcrops with high magnetic intensity consisting a moderate intrusive suite ranging from 32911.2 nT to 32930.1 nT. The northern part of the study area has revealed the extent of granites and their equivalents. While the southern part is characterized by sedimentary basement with many intrusive bodies ranging from 32925.3 nT to 32933.8 nT.

Regional field has thrown some light on the geology and structure of this study area. High-sensitivity aeromagnetic data over the area contain both low-amplitude, linear anomalies produced by structurally deformed magnetized layers near the top of the sedimentary section and high amplitude, broad anomalies produced within the basement. Least square method has been successful in separating the anomalies produced by these two source regions.

5.0 References

[1] Hartman, R. R., D. J. Teskey, and J. L. Friedberg, 1971, A systemfor rapid digital aeromagnetic interpretation: Geophysics, 36,891–918.

[2] Smith, R. S., A. Salem, and J. Lemieux, 2005, An enhanced method for source parameter imaging of magnetic data collected for mineral exploration: Geophysical Prospecting, 53, 655–665.

[3] Henderson, R. G., and I. Zietz, 1948, Analysis of total magnetic intensity anomalies produced by point and line sources: Geophysics, 13, 428–436.

[4] Phillips, J. D., 2000, Locating magnetic contacts: A comparison of the horizontal gradient, analytic signal, and local wave number methods: 70th Annual International Meeting, SEG, Expanded Abstracts, 402–405.

[5] Rahaman MA (1976): Review of Basement Geology of Southwestern Nigeria, Elizaber than Publishing Company, Nigeria pp 41-58

[6] Ajayi O, Adejoke- Anthony C.W (1988): Ground water prospects in the basement complex rock of South west Nigeria: Journal of African Earth Science vol.7 pp227 to 230

[7] Folami SL (1992): Interpretation of Aeromagnetic Anomalies in Iwaraja Area, Southwestern Nigeria. Journal of Mining and Geology 28(2) 391-396

[8] Akinloye MK, Fadipe DO and Adabanija MA (2002): A radiometric mapping of the Ladoke Akintola University Campus, Ogbomoso, Southwestern Nigeria: Science focus vol. 1 pp 51.

[9] Johnson, W.W.(1969).The least-squares method of interpreting magnetic anomalies caused by two-Dimensional structures. Geophysics, 34: 65-74.

[10] Dobrin, M. B. (1976) Introduction to Geophysical Prospecting, McGraw-Hill Book Company, New York, 630p.

[11] Dobrin, M. B. and Savit, C. H. (1988) Introduction to Geophysical Prospecting, Fourth Edition, McGraw-Hill Book Company, New York, 867p.

[12] Weisstein, Eric W. "Least Squares Fitting--Polynomial." From *MathWorld*--A Wolfram

[13] Web Resource. http://mathworld.wolfram.com/LeastSquaresFittingPolynomial.html